Applied Catalysis B: Environmental 150–151 (2014) 619–629

Contents lists available at ScienceDirect

Applied Catalysis B: Environmental

journal homepage: www.elsevier.com/locate/apcatb

Disinfection of real and simulated urban wastewater effluents using a mild solar photo-Fenton

J. Rodríguez-Chueca [a], M.I. Polo-López [b], R. Mosteo [a], M.P. Ormad [a], P. Fernández-Ibáñez [b,*]

[a] Department of Chemical Engineering and Environmental Technologies, University of Zaragoza, 3 María de Luna Street, 50018 Zaragoza, Spain
[b] Plataforma Solar de Almería – CIEMAT, P.O. Box 22, 04200 Tabernas, Almería, Spain

ARTICLE INFO

Article history:
Received 16 September 2013
Received in revised form
10 December 2013
Accepted 16 December 2013
Available online 24 December 2013

Keywords:
E. coli
E. faecalis
Solar photo-Fenton
Compound parabolic collector
Pilot plant

ABSTRACT

This work aims to assess the effectiveness of a mild solar photo-Fenton system (low reagent concentrations and near neutral pH) for the removal of fecal bacteria in urban wastewater effluents. *Escherichia coli* and *Enterococcus faecalis* were simultaneously evaluated in real and simulated effluents at initial concentrations of 10^3 and 10^6 CFU/mL. Several concentrations of ferrous sulfate (2.5–10 mg-Fe^{2+}/L) and hydrogen peroxide (5–50 mg/L) were tested in solar CPC reactors (total volume: 20 L) under natural sunlight. Photo-Fenton results were compared with the bactericidal effects of solar exposure and H_2O_2 under the same experimental conditions. Solar photo-Fenton processes at pH 5 and pH 3 were compared. The results showed complete bacterial inactivation in almost all conditions, but the solar UVA energy dose required to achieve similar results at pH 5 (24–30 kJ/L) was higher than at pH 3 (2–20 kJ/L). This work also shows experimentally that the presence of precipitated iron at near-neutral pH has no benefits for disinfection efficacy; it actually causes a slight decrease in effectiveness under these experimental conditions. *E. faecalis* clearly showed higher resistance than *E. coli* to all treatments (photo-Fenton and H_2O_2/solar) using both naturally occurring and seeded bacteria. The disinfection tests in real effluents showed very promising results despite the complexity and variability of the organic and inorganic matter in the effluents. A 3-log decrease in *E. coli* and *E. faecalis* was attained in real effluents, and a 6-log abatement was observed in simulated wastewater when the solar photo-Fenton process at pH 5 was used. This result has important implications for the treatment of reclaimed wastewater.

1. Introduction

The growth of the world population is accompanied by an increase in industrial, agricultural and recreational activities. These activities, in turn, increase the demand for fresh water. For this reason, in the next few decades, access to clean fresh water sources will be a serious global problem. Water scarcity and the health risks associated with polluted water resources will be major global issues.

The primary purpose of the reclamation and reuse of water is to draw water directly from non-traditional sources, such as industrial or municipal wastewaters, and to restore it to higher quality [1]. Wastewater contains a great diversity of chemical pollutants and pathogens, and it includes a large amount of organic matter, all of which must be removed or transformed into harmless compounds.

Wastewater reuse may provide a new and stable source of water for agriculture, industrial processes, and some domestic uses that do not require potable water. The potential benefits for agriculture, environmental preservation, and energy conservation may be even more important.

The agricultural sector is the largest consumer of fresh water, using 70–95% of it for irrigation. Wastewater reuse in agriculture will reduce stress on the water supplies in semi-arid and very contaminated areas [2]. Guidelines and specific national policies for reclaimed water quality and reuse limit the loads of several waterborne pathogens, such as fecal coliforms and *Escherichia coli* [3–7]. Depending on the final use of the reclaimed water, the maximum allowed concentrations of microbial agents vary; they are more restrictive for urban and agricultural uses and less restrictive for industrial, recreational, and environmental uses. In particular, the guidelines for water recycling, established by different water authorities for unrestricted irrigation, are as follows for *E. coli* and coliforms, in terms of CFU per 100 mL: <1 as defined by the USEPA [3], <1000 as defined by the WHO [4], <10 as defined by Italian rules [5], <1 as defined by Australian guidelines [6] and <100 as defined by Spanish regulations [7].

Urban wastewaters are commonly treated with activated sludge, followed by treatment in sedimentation systems (secondary treatment). Depending on the regulations in each area or

* Corresponding author. Tel.: +34 950387957; fax: +34 950365015.
E-mail addresses: rodriguezchueca@gmail.com (J. Rodríguez-Chueca), pilar.fernandez@psa.es (P. Fernández-Ibáñez).

0926-3373/$ – see front matter © 2013 Elsevier B.V. All rights reserved.
http://dx.doi.org/10.1016/j.apcatb.2013.12.027

country, these wastewater effluents may be able to be discharged to surface waters or used for restricted irrigation and industrial applications. Based on the microbial quality requirements established by various agencies, it is clear that an efficient tertiary treatment of effluents is needed.

Mostly, urban wastewater effluents contain, among other pollutans, high loads of fecal bacteria. Levels of these bacteria are commonly reported in terms of the concentrations of *E. coli*, total coliforms (TC) and fecal coliforms (FC). *E. coli* normally accounts for the majority of the fecal coliform group [8]. The typical quality of these wastewater effluents is approximately 10^3–10^5 TC/100 mL [9–11]. The fecal load limit established by the WHO for unrestricted irrigation uses is ≤1000 CFU of FC/100 mL [4].

Different physicochemical water treatments are currently in use, including treatments with chlorine, UVC, and ozone. Although chlorine is a very strong oxidant and has a residual effect, it may react with natural organic matter (NOM) to form carcinogenic halogenated disinfection by-products (DBP), such as trihalomethanes (THMs) and haloacetic acids (HAA) [12–14]. The use of UVC has limited efficiency against very resistant pathogens [15], it has a non-residual effect, and it requires high capital costs and high operation and maintenance costs. Thus, alternative technologies are being studied for the removal of water pathogens to overcome these limitations. Some advanced oxidation processes (AOPs), such as H_2O_2/UV-C, photocatalysis with titanium dioxide, photo-Fenton processes and H_2O_2/O_3, are being proposed as new approaches for water disinfection [16–22]. The efficacy of AOPs lies in the generation of hydroxyl radicals ($OH^\bullet$). These highly oxidating species can oxidize almost all organic compounds and can inactivate a wide range of microorganisms. Furthermore, the use of solar radiation to promote some AOPs has been demonstrated to be very efficient for water purification, and it has the advantage of relying on an environmentally friendly source of photons [23].

Recently, research has been conducted on mild photo-Fenton and solar radiation with low concentrations of H_2O_2 for water disinfection [21,24]. Photo-Fenton produces hydroxyl radicals via a series of catalytic cycle reactions with iron (Fe^{2+} and Fe^{3+}), H_2O_2 and UV–vis radiation (≤600 nm). These reactions are summarized as follows [25]:

$$Fe^{2+} + H_2O_2 \rightarrow Fe^{3+} + OH^- + OH^\bullet \quad (K = 70\,M^{-1}\,s^{-1}) \tag{1}$$

$$Fe(OH)^{2+} + h\nu \rightarrow Fe^{2+} + OH^\bullet \tag{2}$$

The highest photo-Fenton efficacy is found at pH 2.8 [25] because this pH minimizes the precipitation of iron salts. Nevertheless, photo-Fenton reactions at near-neutral pH values would be desirable to reduce operational costs associated with acidification and neutralization of large volumes of wastewater. Few articles have dealt with this subject [21,26,27]. These papers have reported the successful inactivation of single bacteria (*E. coli* or *Enterococcus faecalis*) in different water matrixes under very different conditions. There is still scarce information about the applicability of this process for the disinfection of real wastewaters under realistic solar conditions.

Solar photo-assisted treatment with H_2O_2 induces accelerated inactivation of several types of microorganisms in water due to photo-chemical and photo-biological processes that occur when solar photons and non-toxic amounts of hydrogen peroxide interact with living cells [20,28,29]. This phenomenon cannot be considered to correspond to any of the well-known AOPs because it does not generate hydroxyl radicals by the photo-chemical reaction of H_2O_2 with sunlight (wavelengths >300 nm) [30]. Our previous research on H_2O_2/sunlight processes for water decontamination has shown that no significant degradation of organic matter occurs during disinfection [24]. It is believed that the mechanism of action of this method is based on the stressing effect produced by H_2O_2 and solar photons due to internal photo-Fenton reactions with the available iron inside the microbial cells [31].

The efficiency of water disinfection strongly depends on water composition and the inhabiting bacterial consortium. The role of organic matter is controversial; some articles report that it provides a beneficial effect for disinfection, and others report that it is detrimental [21,24,27,32]. There are few reports on the removal of bacterial consortia and naturally occurring bacteria in real wastewaters [29,33] using photo-Fenton treatment or H_2O_2/solar treatment.

The aim of this work was to evaluate the efficiency of a solar photo-Fenton process at near neutral pH and a H_2O_2/solar process for removing *E. coli* K-12 and *E. faecalis* simultaneously spiked into simulated municipal wastewater effluents and naturally occurring *E. coli* and *E. faecalis* in real municipal wastewater effluents. Several concentrations of ferrous sulfate (2.5–10 mg-Fe^{2+}/L) and hydrogen peroxide (5–50 mg/L) were evaluated in two solar CPC reactors under natural solar conditions. The effect of pH on solar treatment efficiency was evaluated at pH 3 and pH 5. Furthermore, the influence of precipitated and dissolved iron on the efficiency of the photo-Fenton process at near-neutral pH values was also investigated. A pH level of 7 was not experimentally evaluated, as our previous publications [24,33] showed that the inactivation of *E. coli* and *Fusarium solani* spores by a photo-Fenton process at pH 7 were very similar to those observed for an H_2O_2/solar process. This result was attributed to the fact that no dissolved iron was measured in the samples at this pH.

2. Materials and methods

2.1. Solar experiments

All experiments were conducted at Plataforma Solar de Almeria (PSA) under natural solar radiation on completely sunny days, from April to July 2012 (summer conditions), for 4 h of solar exposure (10:30–14:30, local time).

Three types of solar experiments were performed in this work: (i) H_2O_2/solar treatment and (ii) solar photo-Fenton treatment. Both treatments were performed in simulated effluents (SE) and real effluents (RE) from urban wastewater treatment plants using CPC pilot reactors. (iii) Solar photo-Fenton experiments were conducted to study the effect of the presence or absence of precipitated iron in small stirred vessel reactors in distilled water (DW).

2.1.1. Solar CPC pilot reactors

Most of the experiments were performed in two pilot plants equipped with compound parabolic collector (CPC) reactors (Fig. 1). Both reactors are recirculated batch systems with total volumes of 20 L and illuminated volumes of 14 L in the CPC photo-reactors. The ratio of illuminated volume to total volume is 0.7. The CPC mirrors (total surface area of 1 m^2) are titled at an angle of 37° relative to the horizontal plane, which enhances the solar radiation collection [34]. The flow rate was 10 L/min in both reactors.

The experiments were performed in SE and RE. Water was acidified using sulfuric acid (Merck, Germany, analytical grade) after adding iron salts in the photo-Fenton experiments. Then, the bacterial suspensions were added to the SE, and, finally, the hydrogen peroxide was added. The same procedure was followed in the RE samples, without spiking the bacteria because the naturally occurring *E. coli* and *E. faecalis* were evaluated in those samples.

Samples were taken at predetermined times for a period of 4 h. The 'dark control sample' was the first sample of each experiment kept in the dark at room temperature, which was analyzed at the end of the experiment to examine the effects of the process in the dark on bacteria viability. Temperature (T) (Checktemp, Hanna

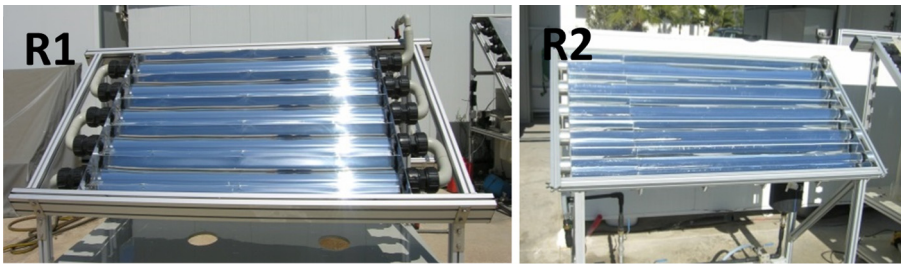

Fig. 1. Solar CPC reactors at the Plataforma Solar de Almería facilities.

instruments, Spain), dissolved oxygen (DO) (Crison Oxi 45+) and pH (multi 720, WTW, Germany) were measured directly in the CPC reactor during the experiments. All experiments were performed at least in duplicate. The results were highly reproducible. To verify the reproducibility, we used one-way ANOVA, $P < 0.05$, confidence >95%, to analyze the measurements (Origin v7.0300, OriginLab Corp., Northampton, USA). The results shown in the graphs represent the averages of the replicates, and the error bars indicate the standard deviations.

2.1.2. Stirred vessel reactors

Special tests were performed to evaluate the effect of the presence or absence of precipitated iron at near neutral pH on the photo-Fenton efficiency for bacterial inactivation. For this purpose, DW was used as the water matrix to avoid any interference of ions and molecules. These experiments were performed in 250 mL DURAN-glass (Schott, Germany) stirred vessel reactors, with 200 mL of DW, 10 mg/L of Fe^{2+} and a pH adjusted to pH 5 using NaOH.

Two reactors (replicates) were prepared under these conditions, other two reactors (replicates) were prepared similarly, but with water that was filtered using 0.2 μm filters CHROMAFIL Xtra PET-20/25 (PANREAC, Spain) after adding the iron salt, pH adjusting to 5 and stirring for 5 min. This filtration was performed to remove the precipitated iron from the water samples. After this, 20 mg/L of H_2O_2 was added to all reactors at the same time, and the bacterial suspensions were added at an initial concentration of 10^6 CFU/mL. Then, the reactors were exposed to natural sunlight for 4 h. Samples were taken and evaluated as described in the bacterial quantification section.

2.1.3. Solar radiation measurement

Proper evaluation of sunlight-driven processes should take into account two variables: (i) the accumulated solar UVA energy received in the solar reactor per unit of treated water volume (Q_{UV}, Eq. (3) [35]), and (ii) the experimental time (t), which plays an important role in the equation for Q_{UV} but also in the kinetics of the solar mechanisms that occur during exposure. For example, in two case studies (on two different days) with the same accumulated Q_{UV}, one case achieved inactivation within 2 h, and the other achieved it in 5 h. These different times lead to very different inactivation kinetics and final disinfection results. For this reason, all experiments were conducted at the same local time, with similar environmental temperatures and similar levels of solar UVA irradiation. The maximum and minimum UVA irradiances were 27.1 (±1.4) W/m^2 and 48.2 (±2.4) W/m^2, respectively, in all experiments presented in this work. The average solar incident UVA irradiances registered during the tests at different times are presented in Fig. 2, and the same irradiation pattern is observed in all cases.

The solar UVA irradiance was measured by using a global UVA pyranometer (295–385 nm, Model CUV4, Kipp & Zonen, Netherlands), with a typical sensitivity of 264 mV/(W/m^2). The pyranometer provides data in terms of incident W/m^2. This is used to calculate the total UV energy received per unit volume, according to Eq. (3):

$$Q_{UV,n} = Q_{UV,n-1} + \frac{\Delta t_n \overline{UV}_{G,n} A_r}{V_t} \quad \Delta t_n = t_n - t_{n-1} \tag{3}$$

where, $Q_{UV,n}$ and $Q_{UV,n-1}$ are the UV energies accumulated per unit volume (kJ/L) at times n and $n-1$, respectively. $UV_{G,n}$ is the average incident irradiation on the irradiated area, Δt_n is the experimental time for the sample, A_r is the illuminated area of the collector (m^2), and V_t is the total volume of treated water (L).

2.2. Water types

Simulated effluent of urban wastewater treatment plant (SE), containing 25 mg/L of dissolved organic carbon (DOC), was used as model wastewaters to investigate the inactivation efficiencies of solar treatments in the absence of the chemical and microbiological fluctuations often observed in real sewage effluents. The SE had the following composition: $NaHCO_3$ (96 mg/L), NaCl (7 mg/L), $CaSO_4 \cdot 2H_2O$ (60 mg/L), urea (6 mg/L), $MgSO_4$ (60 mg/L), KCl (4 mg/L), $CaCl_2 \cdot 2H_2O$ (4 mg/L), peptone (32 mg/L), $MgSO_4 \cdot 7H_2O$ (2 mg/L) and meat extract (22 mg/L) [24].

Real urban wastewater treatment plant effluent (RE) from El Bobar (Almería, Spain) was used as the real urban sewage effluent. The first stage in this plant consists of a pre-grinding step to remove coarse solids. The water is then lifted and subjected to a pre-treatment consisting of grinding, sanding and degreasing. Water from the pre-treatment is directed to a primary settling tank, where the solids are decanted after passing through the secondary treatment. Secondary treatment consists of a biological treatment by activated sludge and subsequent decanting. The same wastewater source effluent has been investigated elsewhere [29,33]. The

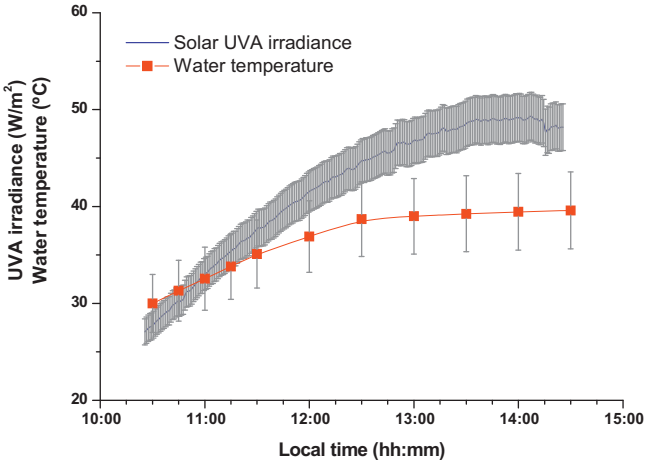

Fig. 2. Average solar UVA irradiance and temperature of water samples over all experiments in the CPC pilot reactors (April–July 2012, 10:30–14:30 local time). Error bars correspond to standard deviations.

Table 1
Physicochemical characteristics of the simulated (SE) and real municipal wastewater treatment plant effluents (RE) used in this study.

	SE	RE
Na^+ (mg/L)	35.80 ± 1.10	211.40 ± 22.80
NH_4^+ (mg/L)	2.70 ± 1.00	32.00 ± 11.70
K^+ (mg/L)	3.40 ± 0.60	33.10 ± 5.80
Mg^{2+} (mg/L)	17.20 ± 0.30	48.00 ± 5.90
Ca^{2+} (mg/L)	21.63 ± 2.30	117.00 ± 10.30
SO_4^{2-} (mg/L)	9.00 ± 1.40	102.60 ± 28.80
Cl^- (mg/L)	11.50 ± 2.10	337.50 ± 10.80
NO_3^- (mg/L)	130.40 ± 7.60	23.50 ± 16.00
PO_4^{3-} (mg/L)	12.10 ± 3.00	17.10 ± 29.80
pH	8.15 ± 0.30	7.53 ± 0.10
Conductivity (μS/cm)	362 ± 12	1458 ± 89.80
Turbidity (NTU)	1.50 ± 0.10	14.60 ± 6.62
DOC (mg/L)	20–30	17.00 ± 3.00
IC (mg/L)	0.5–4	56.50 ± 6.60
E. coli (CFU/mL)	–	10^3
E. faecalis (CFU/mL)	–	10^3

DOC, dissolved organic carbon; DIC, dissolved inorganic carbon.

main physicochemical characteristics of the SE and RE are shown in Table 1.

Ion concentrations were measured by ion chromatography (IC) using a DX-600 model chromatograph (Dionex Corporation, Sunnyvale, California) for anions and a DX-120 model for cations. DOC and dissolved inorganic carbon (DIC) were measured by direct injection of samples filtered with 0.2 μm syringe-driven filters into a Shimadzu – 5050 A TOC analyzer (Shimadzu Corporation, Kyoto, Japan). Turbidity was measured with a turbidimeter Model 2100N, Hach (USA). The natural presence of dissolved iron in the RE was analyzed by spectrophotometry with phenanthroline/acetic acid (UV–vis measurements, detection limit of 0.05 mg/L). No iron was detected in any of the RE water samples with this method.

2.3. *E. coli* and *E. faecalis* enumeration

E. coli strain K12 (CECT 4624) and *E. faecalis* strain CECT 5143 were obtained from the Spanish Culture Collection (CECT). They were used to prepare the bacterial suspensions spiked in the SE. Fresh liquid cultures were prepared in Luria-Bertani nutrient medium (LB Broth, Panreac) and incubated at 37 °C with rotary shaking for 20 h. The bacterial stationary phase concentration was 10^9 CFU/mL. Bacterial suspensions were harvested by centrifugation at 900 × *g* for 10 min. The bacterial pellet was re-suspended in phosphate-buffered saline (PBS) and diluted in the reactor to an initial concentration of 10^6 CFU/mL. The samples taken during the experiments were enumerated using the standard plate counting method, through a serial 10-fold dilutions in PBS; diluted samples of 60 μL were plated on ChromoCult® Coliform Agar (Merck KGaA, Darmstadt, Germany) for *E. coli* and Slanetz & Bartley agar (Scharlau®, Spain) for *E. faecalis*. Colonies were counted after incubation for 24 h at 37 °C. The detection limit (DL) of this experimental method was found to be 2 CFU/mL. For the RE experiments, the naturally occurring *E. coli* and *E. faecalis* concentrations were determined by the same methodology.

2.4. Reagents and analysis

Ferrous sulfate heptahydrate ($FeSO_4{\cdot}7H_2O$, PANREAC, Spain) was used to obtain Fe^{2+} concentrations of 2.5, 5 and 10 mg/L. Water samples were filtered with NY 0.2 μm CHROMAFIL® Xtra PET-20/25 (PANREAC, Spain) to remove the precipitated iron. Then, each sample was mixed with 1 mL of 1,10-phenanthroline (1 g/L) and 1 mL of buffer solution, according to ISO 6332, to measure the dissolved Fe^{2+} and total iron (Fe^T) concentrations, i.e., the concentrations of Fe^{2+} and Fe^{3+}. The colored complex formed was measured with a spectrophotometer (PG Instruments Ltd T-60-U) at 510 nm in glass cuvettes (1 cm path length). Fe^{2+} and Fe^T concentrations were determined using corresponding calibration curves. The concentration ratios of Fe^{2+}:H_2O_2 used were 1:2 and 1:5; with Fe^{2+} concentrations of 2.5, 5 and 10 mg/L and H_2O_2 concentrations of 5, 10, 20, 25 and 50 mg/L.

Hydrogen peroxide (35%, w/v aqueous solution) was obtained from Merck and diluted directly into the water samples from 5 to 50 mg/L for the H_2O_2/solar, photo-Fenton and Fenton experiments. H_2O_2 concentration was measured in a spectrophotometer (PG Instruments Ltd T-60-U) at 410 nm in glass cuvettes (1 cm path length) according to DIN 38409 H15, based on the formation of a yellow complex from the reaction of titanium (IV) oxysulfate with H_2O_2. The titanium (IV) oxysulfate method has a 0.1 mg/L detection limit. The signal was read after 5 min of incubation and compared to a H_2O_2 standard curve that was linear in the range of 0.1–100 mg/L H_2O_2. The titanium (IV) oxysulfate solution (Riedel-de Haën, Germany) was used as received. Catalase was added to the water samples to eliminate residual hydrogen peroxide: 1-mL samples were mixed with 100 mL of 2300 U/mg bovine liver catalase at 0.1 g/L (Sigma Aldrich, USA).

3. Results

3.1. H_2O_2/solar radiation

Fig. 3(a and b) shows the simultaneous inactivation of *E. coli* and *E. faecalis* in SE by treatment with H_2O_2 (5, 10, 20, 25 and 50 mg/L) and solar radiation at pH 5 for 4 h. In the case of *E. coli*, the detection limit was reached with all H_2O_2 concentrations except 5 mg/L. The greatest inactivation was found for 50 mg/L of H_2O_2, which had an accumulated solar UV dose of 21.7 kJ/L. For *E. faecalis*, the inactivation was slower than for *E. coli*, and only treatment with 50 mg/L H_2O_2 reached the limit of detection; in this case, a greater amount of solar energy was received: 36.7 kJ/L of Q_{UV}. The direct oxidative effect of H_2O_2 (the highest concentration of H_2O_2 tested: 50 mg/L) on viability was very low for both bacteria compared to the synergistic effect of H_2O_2 and solar radiation (dark controls in Fig. 3), and the inactivation curve shows a shape very different from that found when H_2O_2 and solar radiation are applied simultaneously.

The parameters pH, DO and DOC were measured during the solar tests (Table 2). The pH remained nearly constant at 5 during the experiments. No significant DOC reduction was observed in any case. H_2O_2 was monitored throughout the experiments; a slight reduction in H_2O_2 (<10%) was observed at the end of the experiments.

Other control experiments were conducted in the dark in the CPC reactor using re-circulation without H_2O_2, and these showed no significant decrease in *E. coli* or *E. faecalis* (data not shown). Thermal inactivation of *E. coli* during the experiments was ruled out by the control tests conducted in the dark at pH 3 and 5 with temperature increasing from 25 °C to 44 °C (as in the solar photo-Fenton experiment, but in the absence of radiation). As expected, there was no detrimental effect on bacterial survival under these pH and temperature conditions (data not shown). This result allows us to disregard any thermal or mechanical effects as explanations for the inactivation curves in Fig. 3.

3.2. Photo-Fenton processes at pH 3 and 5

3.2.1. Photo-Fenton process at pH 5

This part of the study considers the photo-Fenton process at pH 5 because this pH value is a compromise between the optimal pH value for photo-Fenton process, pH 2.8 [25], and the neutral pH (7–8) of natural waters and wastewater discharges.

Table 2
Initial (i) and final (*f*) values of pH, DO and DOC for the experiments using SE samples. The last column shows whether the detection limit (DL = 2 CFU/mL) was reached at any time during the experiment. Q_{UV} shows the accumulated solar UV irradiation per unit volume after 4 h of treatment.

Conc. (mg/L)	Fig.	pH	DOC reduction (%)	Dissolved Fe_i^T/Fe_f^T (mg/L)	Q_{UV} (kJ/L)	DL
(H_2O_2)				*H_2O_2/solar at pH 5*		
5	3	5.1	–	–	32.4	NO
10	3	4.9	–	–	32.3	*E. coli*
20	3	5.3	–	–	35.0	*E. coli*
25	3	4.9	–	–	32.4	*E. coli*
50	3	5.1	–	–	36.7	YES
(Fe–H_2O_2)				*Solar photo-Fenton at pH 5*		
2.5–5	4	5.1	–	0.2/0.1	35.1	NO
5–10	4	5	–	0.2/0.0	36.9	NO
5–25	4	5	–	1.0/0.1	34.8	*E. coli*
10–20	4	4.9	19	0.5/0.2	35.6	*E. coli*
10–50	4	4.9	22	0.14/0	34.8	YES
(Fe–H_2O_2)				*Solar photo-Fenton at pH 3*		
2.5–5	6	2.9	28	0.9/0.6	32.6	YES
5–10	6	3	51	2.9/1.2	34.1	YES
10–20	6	3.1	69	6.5/2.6	37.1	YES
10–50	6	3	70	7.5/1.0	35.2	YES
(Fe)				*Fe^{2+}/Solar*		
10	5	5.2	8	6.0/4.5	33.8	NO

DOC: Dissolved Organic Carbon, no data are shown if reduction was below the detection limit of DOC measurement.
Dissolved Fe_i^T/Fe_f^T = total (Fe^{2+} and Fe^{3+}) dissolved iron (mg/L) in the initial and final samples.
Q_{UV}: solar UV-A radiation accumulated in the sample during treatment.
DL: Detection limit.

Fig. 4a shows the inactivation of *E. coli* by the photo-Fenton process at pH 5 using several Fe^{2+} and H_2O_2 concentrations: 2.5/5, 5/10, 5/25, 10/20 and 10/50 mg/L. A 6-log reduction (reaching the DL) was observed for the cases of 10/50, 10/20 and 5/25 mg/L of Fe^{2+}/H_2O_2, with 24.71, 30.35 and 34.77 kJ/L of Q_{UV}, respectively. Lower reagent concentrations (2.5/5, 5/10) showed a 4.5-log decrease after 4 h of solar treatment. Fenton tests were performed in the same reactor in the dark for the two highest concentrations tested in this work: 10/20 and 10/50 mg/L of Fe^{2+}/H_2O_2. Reductions of 1- and 5-log, respectively, were observed in *E. coli*. The high inactivation at 10/50 mg/L of Fe^{2+}/H_2O_2 is due not only to the Fenton reaction (Eq. (1)) but also the germicidal effect of 50 mg/L H_2O_2, which was already shown in Fig. 3a.

The inactivation of *E. faecalis* under similar photo-Fenton conditions is shown in Fig. 4b. Lower inactivation rates were observed for *E. faecalis* than for *E. coli* in all cases. The DL was only reached with the highest tested concentrations: 10 mg/L of Fe^{2+} and 50 mg/L of H_2O_2. These conditions required 29.77 kJ/L of Q_{UV}. Lower photo-Fenton reagent concentrations yielded 2.5- to 4-log decreases. Fenton (dark) inactivation with 10/20 and 10/50 mg/L of Fe^{2+}/H_2O_2 leads to 0.5- and 2.7-log reduction, respectively.

The total dissolved iron concentration (Fe^T) in the reactor was measured every hour in all experiments. The amounts of iron added were 2.5, 5 and 10 mg/L, and the initial Fe^T values measured were in the range of 0.1–1 mg/L (Table 2), which means that most of the added iron was precipitated as ferric hydroxide (pH 5) in all cases. The H_2O_2 consumption after 4 h of photo-Fenton treatment was in the range of 75–98%. No significant DOC reduction was observed for the three lower concentrations, but a DOC reduction of approximately 20% was measured for 10/20 and 10/50 mg/L of Fe^{2+}/H_2O_2.

Solar photo-inactivation of both bacteria in the SE was evaluated in the same CPC reactors conditions in the presence or absence of Fe^{2+} (10 mg/L). A moderate detrimental effect was expected due to the action of solar UVA photons and UVA/Fe [21,36]. The results (Fig. 5) showed a 3-log and 5-log decrease induced by solar radiation for 4 h for *E. faecalis* and *E. coli*, respectively. As expected, the residual bacteria concentrations remain in the reactor regardless of the treatment time. In contrast, the addition of 10 mg/L of Fe^{2+} produced a clear enhancement, mainly for *E. faecalis*, although the DL was not reached for either of the bacteria.

3.2.2. Solar photo-Fenton process at pH 3

Complete inactivation of *E. coli* and *E. faecalis* was obtained with a solar photo-Fenton process at pH 3 at all tested concentrations of Fe^{2+}/H_2O_2: 2.5/5, 5/10, 10/20 and 10/50 mg/L (Fig. 6a and b). The viabilities of both bacteria at pH 3 were tested in the reactor in the dark, and no significant decrease (<1-log) was observed after 3 h. To ensure proper homogenization of the reagents and bacterial suspensions in the reactor, the first 10 minutes of the experiment were conducted in the dark. The Fenton reaction occurred during these 10 min (Eq. (1)). $OH^{\bullet}$ radicals generated by this reaction are responsible for the losses of viability observed at this time point. A very small bacterial decrease was observed in *E. faecalis* in all cases; nevertheless, *E. coli* was more sensitive to the Fenton reaction, and 0.5-log to 3-log decreases were observed as the reagents concentrations were increased. Furthermore, the Fenton process was evaluated at 10/20 mg/L of Fe^{2+}/H_2O_2 at pH 3. For *E. coli*, the Fenton results confirm our findings for the photo-Fenton process with the same reagents and conditions in the dark for the first 10 min, i.e., there was a 2-log drop. The Fenton reaction results in a gradual decrease in bacterial concentration (3-log after 4 h), which is much slower than the solar photo-Fenton inactivation curve. *E. coli* concentrations after Fenton treatment are above the DL (Fig. 6a). For *E. faecalis*, the effect of the Fenton reaction was almost negligible in the first 10 min; these bacteria showed resistance to the treatment for the first 2 h, followed by a sharp decrease of nearly 5-log at the end (4 h) of the experiment (Fig. 6b). The *E. faecalis* Fenton kinetics show a very different shape compared to the solar photo-Fenton kinetics, which explains why the final disinfection performance was worse for the Fenton reaction alone.

For both bacteria, the fastest inactivation curve was found at 10/50 mg/L of Fe^{2+}/H_2O_2, with 1.65 kJ/L of Q_{UV} (Fig. 6a) for *E. coli* and 20.68 kJ/L of Q_{UV} for *E. faecalis* (Fig. 6b). For lower reagent concentrations, higher Q_{UV} values were required to reach the DL. Moreover, in the case of *E. faecalis*, no significant differences were observed among all tested concentrations (Fig. 6b). Clearly, the photo-Fenton process is enhanced at pH 3 compared to pH 5 because pH 3 results in much faster bacterial inactivation. Along the same lines, the DOC reduction observed at pH 3 was substantially higher than at pH 5, with a maximum reduction of 70% at 10/50 mg/L of Fe^{+2}/H_2O_2 (Table 2). In terms of DOC, we observed

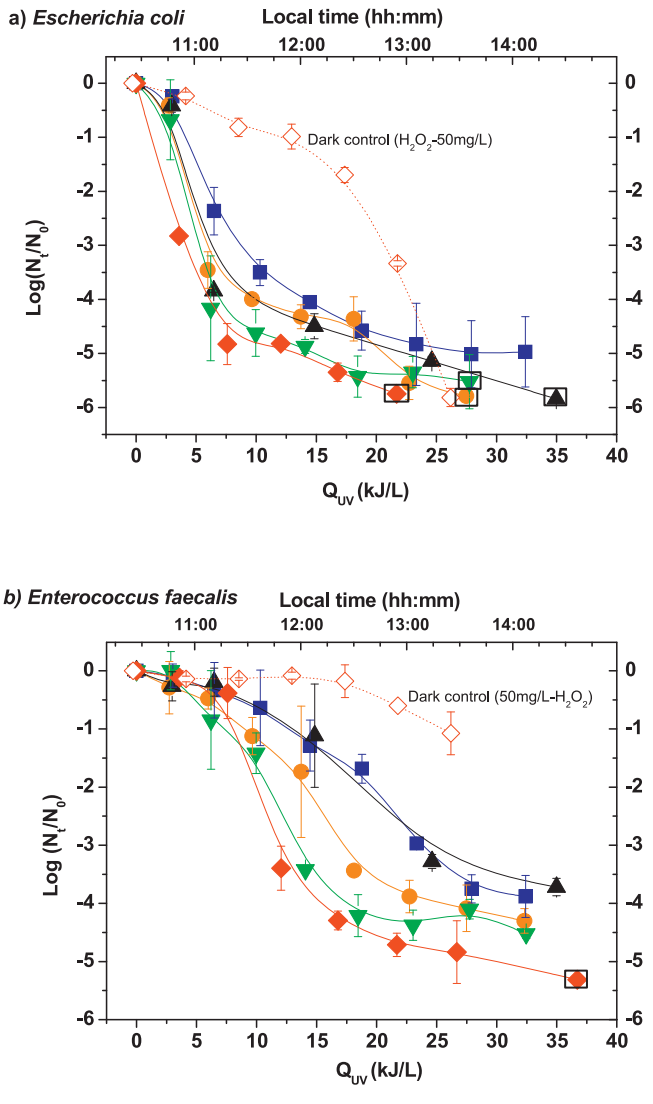

Fig. 3. Inactivation of (a) *E. coli* and (b) *E. faecalis* in SE with H_2O_2/solar radiation at pH 5 and different concentrations of H_2O_2: 5 mg/L (■); 10 mg/L (●); 20 mg/L (▲); 25 mg/L (▼), 50 mg/L (♦) and dark control with 50 mg/L (◇). Open squared symbols (□) were used to indicate that the detection limit (2 CFU/mL) was reached in the experiment.

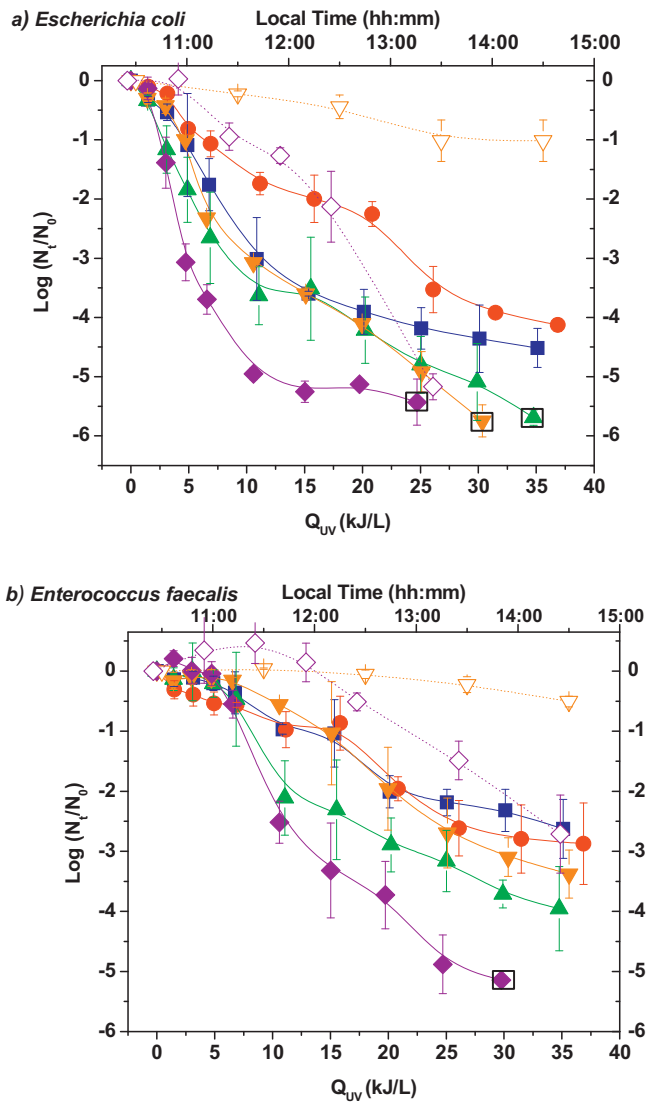

Fig. 4. Inactivation of (a) *E. coli* and (b) *E. faecalis* in SE using solar photo-Fenton at pH 5 at several Fe^{2+}/H_2O_2 concentrations: 2.5/5 mg/L (■); 5/10 mg/L (●); 5/25 mg/L (▲); 10/20 mg/L (▼); 10/50 mg/L (♦). Dark Fenton reactions are sown at Fe^{2+}/H_2O_2 concentrations: 10/20 mg/L (▽) and 10/50 mg/L (◇). Open squared symbols (□) were used to indicate that the detection limit (2 CFU/mL) was reached in the experiment.

that higher reagent concentrations resulted in greater DOC reduction.

Fe^T and H_2O_2 concentrations were measured every hour and every 30 min, respectively. Fe^T decreased during the first hour of the experiment, to approximately 30–50%, and it remained constant at that level until the end of the experiment. H_2O_2 was totally consumed during the first 2 h of the experiment (Table 2).

3.3. Evaluation of precipitated iron in the photo-Fenton process

Two types of experiments were performed to evaluate the effects of precipitated iron in comparison with dissolved iron on photo-Fenton efficiency at near neutral pH. One type of experiment used DW with iron salts (10 mg/L of added Fe^{2+}) and H_2O_2 (20 mg/L) at pH 5 and spiked-in *E. coli* and *E. faecalis* together (the so-called 'non-filtered' tests). These experiments were run simultaneously with the other type of experiment, which used the same photo-Fenton conditions but used water that was filtered prior to adding the bacteria (the 'filtered' tests). Both experiments (200 mL total volume) were exposed to non-concentrated solar radiation in stirred vessel reactors.

The effects of precipitated iron (Fe^P) and dissolved iron (Fe^D) on the photo-Fenton efficiency for *E. coli* and *E. faecalis* inactivation are shown in Fig. 7. The added reagent concentration was 10 mg/L of Fe^{2+}, with 20 mg/L of H_2O_2, and the pH was adjusted to 5 to be close to that of the mild photo-Fenton conditions (close to neutral pH) used for the final applications of this process for water treatment. This condition favored the precipitation of a high percentage of the iron initially added. The dissolved iron concentration was 0.05 mg/L; the rest of the iron may have precipitated as relatively inactive hydrous oxyhydroxides, imparting an orange–brown shade to the water [25]. In contrast, the pre-filtered samples showed no color in the water because the precipitated iron was removed by filtration. No significant differences in the inactivation of *E. coli* were observed, but for the inactivation of *E. faecalis*, the filtered samples were inactivated faster than the unfiltered ones (Fig. 7).

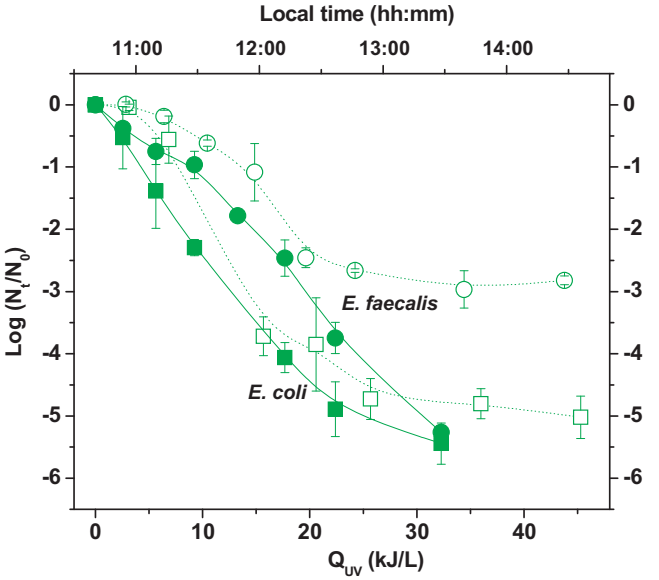

Fig. 5. *E. coli* and *E. faecalis* in SE viability evolution in the CPC reactor under solar light alone (□, ○), and with added 10 mg/L-Fe^{2+} (■, ●).

The results for *E. faecalis* demonstrate that Fe^{D} is more efficient. Bottles with filtered water reached the detection limit faster than bottles with unfiltered water. These results show that the presence of precipitated iron in the water samples does not provide extra hydroxyl radicals via photo-Fenton reactions. On the contrary, the precipitated iron blocks some of the light entering the reactor, decreasing the inactivation efficiency, as shown for *E. faecalis* inactivation in the unfiltered water sample.

3.4. Disinfection of real municipal wastewater effluents (RE)

Fig. 8a and b shows the inactivation of naturally occurring *E. coli* and *E. faecalis* within 4 h of solar photo-Fenton treatment at pH 5. The initially added reagents were 10 mg/L of Fe^{2+} with 20 or 50 mg/L of H_2O_2. In addition, blank experiments testing H_2O_2/solar radiation (10 and 50 mg/L) and Fe^{2+}/solar radiation (10 mg/L) treatments were performed for the RE samples.

All solar treatments led to complete *E. coli* removal (DL = 2 CFU/mL) (Fig. 8a). Nevertheless, small differences in the required solar UV energy dose (between 7 and 15 kJ/L of Q_{UV}) were observed between different solar treatments; Fe^{2+}/solar radiation was exceptional in requiring 31.29 kJ/L of Q_{UV}. The different treatments can be ranked in order of their activation kinetics: 50 mg/L-H_2O_2/solar radiation (7.4 kJ/L of Q_{UV}) > solar photo-Fenton with 10/50 mg/L of Fe^{2+}/H_2O_2 (8 kJ/L of Q_{UV}) > 20 mg/L-H_2O_2/solar radiation (12 kJ/L of Q_{UV}) > solar photo-Fenton at 10/20 mg/L of Fe^{2+}/H_2O_2 (13.1 kJ/L of Q_{UV}) > 10 mg/L-Fe^{2+}/solar radiation (31.3 kJ/L of Q_{UV}). The *E. coli* inactivation rate was faster in both H_2O_2/solar radiation treatments than in the solar photo-Fenton treatments, most likely because the amount of iron dissolved was very small in the photo-Fenton treatments. Table 3 summarizes the Fe^{T} and H_2O_2 concentrations measured throughout the solar experiments. The initial dissolved concentration of Fe^{T} decreased during the first hour of the experiment approximately 80–90% in the photo-Fenton treatments, remaining constant until the end of the process. With treatment by Fe^{2+}/solar radiation, the concentration of Fe^{T} decreased during the first three hours approximately 90%. In addition, H_2O_2 was totally consumed during the first 2 h of the photo-Fenton process, and it remained constant in the H_2O_2/solar radiation treatments.

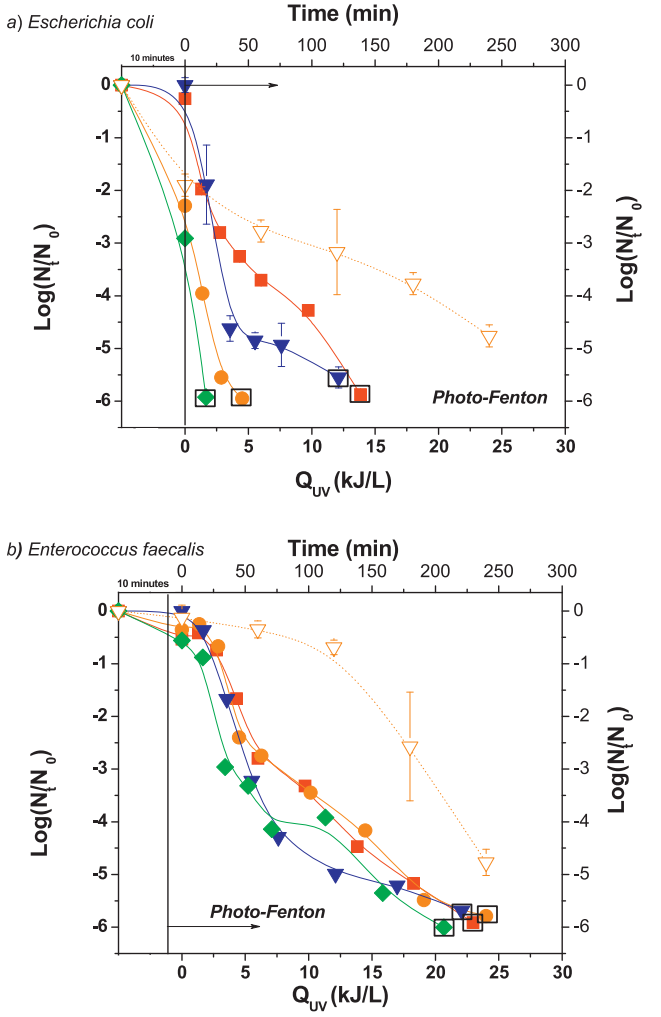

Fig. 6. Inactivation curves of (a) *E. coli* and (b) *E. faecalis* in SE using solar photo-Fenton at pH 3 (prior 10 min Fenton in the dark) at Fe^{2+}/H_2O_2 concentrations of 2.5/5 mg/L (■), 5/10 mg/L (▼), 10/20 mg/L (●), and 10/50 mg/L (◆). Dark Fenton reactions are sown at Fe^{2+}/H_2O_2 concentration of 10/20 mg/L (▽). Open squared symbols (□) were used to indicate that the detection limit (2 CFU/mL) was reached in the experiment.

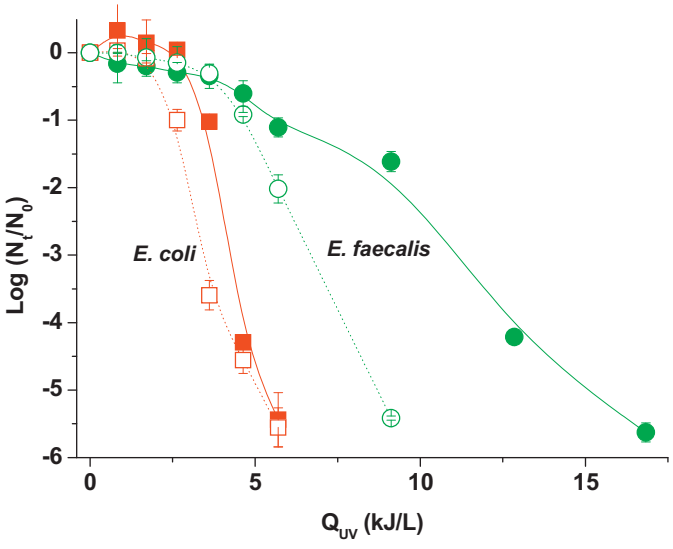

Fig. 7. *E. coli* (■, □) and *E. faecalis* (●, ○) evolution under solar photo-Fenton at pH 5, with 10/20 mg/L of Fe^{2+}/H_2O_2 in bottle reactors: unfiltered (full symbols) and filtered water (open symbols).

Table 3
Initial (i) and final (*f*) values of pH, DO and DOC for the experiments using RE samples. The last column shows whether the detection limit (DL = 2 CFU/mL) was reached at any time during the experiment. Q_{UV} shows the accumulated solar UV irradiation per unit volume after 4 h of treatment.

Conc. (mg/L)	Fig.	pH	DOC reduction (%)	Dissolved Fe_i^T/Fe_f^T (mg/L)	Q_{UV} (kJ/L)	DL
(H_2O_2)				*H_2O_2/solar at pH 5*		
20	8	5.2	8.3	–	34.9	*Yes*
50	8	4.9	10.6	–	34.1	*Yes*
(Fe–H_2O_2)				*Solar photo-Fenton at pH 5*		
10–20	8	5.2	32.5	12/0.3	37.4	*Yes*
10–50	8	4.7	59.3	15/0.2	37.0	*Yes*
(Fe)				*Fe^{2+}/solar*		
10	8	5	1	6.7/0.5	36.0	*Yes*

DOC: Dissolved Organic Carbon, no data are shown if reduction was below the detection limit of DOC measurement.
Dissolved Fe_i^T/Fe_f^T = total (Fe^{2+} and Fe^{3+}) dissolved iron (mg/L) in the initial and final samples.
Q_{UV}: solar UV-A radiation accumulated in the sample to achieve the detection limit after treatment.
DL: Detection limit.

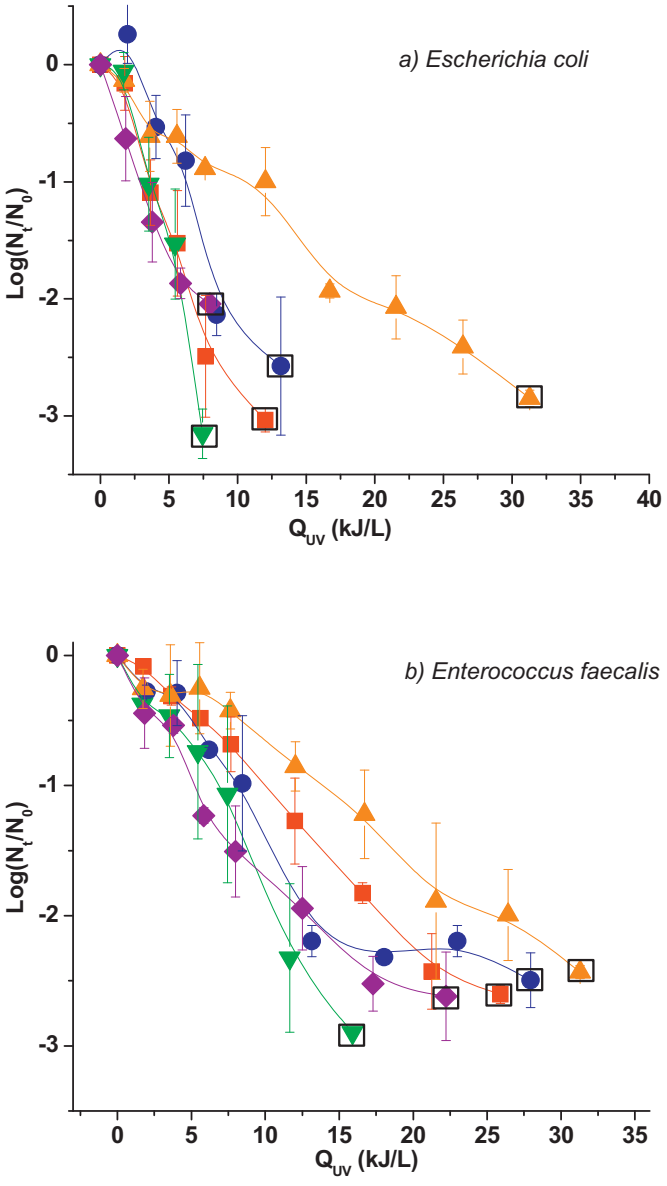

Fig. 8. Comparison of inactivation levels on a) *Escherichia coli* and b) *Enterococcus faecalis* in RE after the application of different treatments: 20 mg/L H_2O_2, pH 5 (■); Solar photo-Fenton 10 mg/L Fe^{2+}, 20 mg/L H_2O_2, pH 5 (●); 10 mg/L Fe^{2+}, pH 5 (▲); 50 mg/L H_2O_2, pH 5 (▼); Solar photo-Fenton 10 mg/L Fe^{2+}, 50 mg/L H_2O_2, pH 5 (◆). Open squared symbols (□) were used to indicate that the detection limit (2 CFU/mL) was reached in the experiment.

The inactivation results for *E. faecalis* were similar to those observed for *E. coli* (Fig. 8b), although greater differences in accumulated solar UV accumulated were found for *E. faecalis* compared to *E. coli*. The inactivation order was as follows: 50 mg/L-H_2O_2/solar radiation (15.9 kJ/L of Q_{UV}) > solar photo-Fenton at 10/50 mg/L of Fe^{2+}/H_2O_2 (22.2 kJ/L of Q_{UV}) > 20 mg/L-H_2O_2/solar radiation (25.9 kJ/L of Q_{UV}) > solar photo-Fenton at 10/20 mg/L of Fe^{2+}/H_2O_2 (27.9 kJ/L of Q_{UV}) > 10 mg/L-Fe^{2+}/solar radiation (31.3 kJ/L of Q_{UV}).

The reduction of DOC was remarkable in the photo-Fenton experiments, reaching 59.3% with 10/50 mg/L of Fe^{2+}/H_2O_2, and reaching 32.5% with 10/20 mg/L of Fe^{2+}/H_2O_2 (Table 3).

4. Discussion

The effects of organic and inorganic chemical compounds in the water were investigated by comparing SE and RE samples. Table 1 shows the anions and cations present in the different water matrixes. Carbonate (CO_3^{2-})/bicarbonate (HCO_3^-) in water may be a limiting factor during photocatalytic processes because these anions can react with OH•, resulting in OH• scavenging that inhibits the oxidative attack [37,38]. Other anions present in the water, such as sulfates, nitrates, chlorides and phosphates, may react with iron, H_2O_2 or other reactive oxygen species (ROS), thereby limiting the amount of OH• (Eq. (1)) available for oxidizing bacteria and organic matter during the photo-Fenton treatment.

Moreover, the presence of dissolve organic matter (DOM) also affects the photocatalytic efficiency. It has been reported that natural organic matter (NOM) has a positive effect on the photo-Fenton process at near-neutral pH when it is used for the inactivation of water pathogens [26,39–42]. Spuhler et al. investigated the effect of resorcinol on *E. coli* inactivation in a photo-Fenton system. They found that the presence of resorcinol enhances the inactivation kinetics compared to reactions run without this organic compound. They suggested that the formation of photo-active Fe^{3+} or Fe^{2+}-resorcinol complexes could favor the inactivation process [21].

DOM can be a highly complex mixture of organic compounds generated by the decomposition and bio-processing of macrocellular structures. The effects of DOM could be different depending on the types of organic compounds generated and naturally present in different waters. Therefore, the effect of DOM on photocatalytic efficiency could vary substantially. Although a deep and complete organic chemical characterization of real wastewater effluents is very difficult, it is well known that some organic acids, such as oxalic, carboxylic, humic and fulvic acids and other intermediates, have significant effects on the photodegradation of a variety of pharmaceuticals through a number of processes [43–45]. DOM can absorb solar radiation, promoting the singlet-excited state, ^{1}DOM*, which then transitions to the ground state or crosses to the

longer-lived excited triplet state $^3DOM^*$ and produces ROS, such as excited singlet oxygen ($^1O_2$), superoxide/hydroperoxyl radicals ($O_2^{-\bullet}/HO_2^{\bullet}$) and $OH^{\bullet}$. The excited triplet state can also act as a photosensitizer, transferring energy directly to the molecules and enhancing the chemical degradation [43–45]. Nevertheless, the presence of DOM has also been observed to decrease the rate of photodegradation by acting as a sunlight filter [46].

Furthermore, in the photo-Fenton case, iron and H_2O_2 react with organic matter (quenchers, scavengers or other molecules). As a result, carboxylic and dicarboxylic acids could be generated, and they could react with iron to form ligand radicals [21,23,25]:

$$Fe^{3+}-(L)_n + h\rightarrow\ Fe^{2+}-(L)_{n-1} + L_{ox}^{\bullet} \quad (4)$$

Fe^{2+} and the radicals generated may also react with O_2, leading to ROS formation. This reaction could be especially important at pH > 3, where Fe^{3+} tends to precipitate. Fe^{3+} organo-complexes play an important role in determining the efficiency of photo-Fenton systems at near neutral pH [21]. Therefore, it is very important to know the nature and chemical composition of the DOM.

The inactivation results for *E. coli* and *E. faecalis* (Fig. 8a and b) in RE samples at pH 5 were significantly better than those obtained in the SE samples (Fig. 4a and b). These results indicate that the DOM present in the RE samples improves the solar photo-chemical process efficiency in all treatments.

The inactivation results show that *E. faecalis* is more resistant than *E. coli* to the effects of the solar treatments. This difference may be attributed to the different architectures of the cytoplasmatic membranes in Gram-negative (*E. coli*) and Gram-positive (*E. faecalis*) bacteria. Gram-negative bacteria have a cytoplasmic membrane, a thin peptidoglycan layer and an outer membrane containing lipopolysaccharide. Gram-positive bacteria have only a cytoplasmic lipid membrane. Their peptidoglycan layer is thicker than that of Gram-negative bacteria. Some reports indicate that complete bacterial inactivation by photocatalysis requires a large number of oxidative attacks by $OH^{\bullet}$ [47–51].

Van Grieken et al. reported that osmotic stress is a factor that affects the inactivation of *E. coli* differently than the inactivation of *E. faecalis* in distilled water and simulated municipal wastewaters [52]. Despite the more complex external structure of Gram-negative bacteria, osmotic stress may induce greater weakening of the *E. coli* cell wall, enhancing the permeability to oxidizing species. This effect would make the *E. coli* cells highly susceptible to oxidative damage. The osmotic stress induced by distilled water was also shown to be a critical factor affecting *E. coli* photocatalytic disinfection by Sichel et al. [19].

Nevertheless, a number of papers also show that *E. coli* is more resistant than *E. faecalis* to TiO_2 photocatalytic treatment. They attribute this resistance to (i) the presence of the outer membrane, which adds an extra wall to protect against oxidative agents [53–56]; (ii) the absence of an outer membrane in Gram-positive bacteria, which makes it easier for hydroxyl radicals to damage the bacterial DNA; and (iii) differences in the chemical composition of the cell wall and protection mechanisms between the two bacteria [57].

However, our results clearly show that *E. faecalis* is more resistant than *E. coli* to all solar treatments that we tested. This greater resistance is most likely due to the thicker cell wall of *E. faecalis*, combined with the different internal defense mechanisms of the bacterium. Nevertheless, we only evaluated two strains, so we cannot draw general conclusions about the relative susceptibilities of Gram-positive and Gram-negative bacteria. Further research should clarify this point. For the first time, our results show higher resistance of naturally occurring *E. faecalis* compared to natural *E. coli* present in RE against the solar photo-Fenton treatment and H_2O_2/solar treatment.

The bacterial inactivation that occurs during photo-Fenton treatment can be attributed to three mechanisms: (i) the generation of external $OH^{\bullet}$ radicals (Eqs. (1) and (2)); (ii) the diffusion of Fe^{2+} inside the cells, where the increased internal iron concentration causes the generation of $OH^{\bullet}$ via internal Fenton reactions between iron and metabolic H_2O_2; and (iii) the direct or indirect oxidation of lipids, proteins, sugars, and DNA, and site-specific oxidation by the iron [58]. The type of iron salt (Fe^{2+} or Fe^{3+}) used for photo-Fenton treatment may affect the inactivation results, as shown by Polo-López et al. [59]. However, in this case, both bacteria were evaluated under the same conditions. Therefore, differences in their inactivation should be due to differences in their internal defense mechanisms because iron could diffuse into both types of cells.

Iron plays a very important role in cell homeostasis. In *E. coli*, a number of chelating compounds are involved in the transport of this metal through the outer membrane, including citrate, ferrichrome, enterobactin, aerobactin, yersiniabactin, and heme. These chelators are transported across the membrane by highly specific proteins of the ABC transport systems. Similar transport mechanisms occur in the cell wall of *E. faecalis*. In both bacteria, the transcription of transport protein genes is regulated by the *Fur* protein. Some authors report that *Fur* mutant cells permit a permanent influx of iron, which overwhelms the iron storage capacity of the cells, leading to intracellular iron overload and oxidative stress sensitivity [60]. Iron metabolism dysregulation in *Fur* mutant cells produced a 2.5-fold iron overload in *E. coli* [61]. When an oxidative treatment (like photo-Fenton treatment) affects the defense and regulatory metabolic systems of bacterial cells, an overload of iron inside the cells will eventually occur. The observed higher resistance of *E. faecalis* to photo-Fenton treatment and solar treatment may be due to a better capacity to respond to this iron overload. López et al. reported that cultures of *E. faecalis* exposed to excess iron for 6 h (0.5 mM $FeCl_3$–NTA) show a significant decrease in the amount of total glutathione, which is associated with an increase in transcription of the genes encoding superoxide dismutase (sodA), catalase (katA), thioredoxin (trx), hydroperoxide resistance protein (ohrA and ohrB) and peptide methionine S-sulfoxide reductase (msrA). Therefore, under an excess of iron, the transcriptional response of *E. faecalis* includes a general oxidative stress response [62]. Bronstein et al. reported that cultures of *E. faecalis* grown under excess iron (0.5 and 1 mM of $FeCl_3$–NTA) increase their intracellular iron content with no changes in cell viability, which suggests that *E. faecalis* can adapt to high-iron conditions and can regulate its iron needs to avoid the effects of iron overload [63]. This ability may explain the greater resistance of *E. faecalis* to photo-Fenton oxidative stress compared to *E. coli*.

Few works have investigated the effect of pH on the disinfection efficiency of photo-Fenton treatment [24,27,59]. Recently, research has focused on the use of photo-Fenton processes for real wastewater treatment at near neutral pH, with the aim of avoiding acidification (pH 2.8) before photo-Fenton treatment and neutralization (pH 6–8) afterward. Neutralization is typically required to make the effluents more environmentally friendly. Avoiding acidification and re-neutralization would reduce the reagent costs and number of treatment steps [21,64].

Moreover, when photo-Fenton treatment is used for disinfection at the optimal pH (2.8), the acidic pH has a very negative effect on the viability of some pathogens (like *E. coli* and related bacteria), so the observed inactivation of microorganism may be due to the low pH rather than the solar treatment.

If we compare the results at pH 3 (Fig. 6) and pH 5 (Fig. 4) in SE, we see that pH 3 produced 3-log and 0.5-log reductions for *E. coli* and *E. faecalis*, respectively, before the solar experiment was started, within the first 10 min. As expected, the photo-Fenton

treatment at pH 3 caused a rapid decrease in both types of bacteria for all conditions studied, bringing the bacteria levels below the detection limit (Fig. 6) with UVA energy dosages (Q_{UV}) lower than those required at pH 5 (Fig. 4). A pH of 3 is very close to the optimal photo-Fenton pH, and at pH 5, most of the active iron is lost from the solution due to precipitation (Table 2). Even though photo-Fenton treatment is not optimized at pH 5, the promising results at this pH show that the presence of only a small amount of dissolved iron can produce enough oxidative damage to achieve complete inactivation of bacteria (below the DL), opening up new possibilities for the treatment of real wastewaters at near-neutral pH.

The influence of the precipitated iron at pH 5 was also experimentally evaluated (Fig. 7). The results clearly show that the precipitated iron negatively affected the inactivation results, especially in *E. faecalis*. For *E. coli*, the results showed no significant differences in the presence and absence of precipitated iron. Precipitated iron screens sunlight; therefore, the generation of hydroxyl radicals could be limited by the iron, causing the inactivation efficacy to decrease. This is clearer in the case of *E. faecalis* because it is more resistant to photo-Fenton treatment than the highly sensitive *E. coli*. In the case of *E. coli*, although the precipitated iron may limit the generation of radicals, the limited oxidative action of the process still produces lethal damage in the *E. coli* cells, leading to complete inactivation.

The accelerated photo-inactivation of microorganisms in water due to the presence of small amounts of hydrogen peroxide is remarkably important. The phenomenon has been demonstrated in several works in recent years [20,21,26,28,65]. Most of these investigations have been carried out in simple waters, such as DW, DW with added organic or inorganic compounds, well water and even simulated municipal wastewater effluents. Additionally, this process has been studied with bacteria such as *E. coli* [21,26], *Bacillus* spores [65] and the fungus *Fusarium* spp. [28,66]. Bichai et al. tested the efficiency of H_2O_2-aided solar disinfection using 5 and 10 mg/L in 1.5-L PET bottles and 20-L batch borosilicate glass reactors equipped with CPCs. They demonstrated the inactivation of naturally occurring *E. coli* in RE during 5 h of solar exposure [29]. Agulló-Barcelo et al. also demonstrated very good inactivation results for several human waterborne pathogens (*E. coli*, spores of sulfite-reducing clostridia, somatic coliphages and F-specific RNA bacteriophages) with 20 and 50 mg/L of H_2O_2 in flow solar CPC-reactors. These authors did not see a marked difference in *E. coli* inactivation between the different concentrations of H_2O_2 [33]. Our results in RE for *E. coli* and *E. faecalis* agree with these findings, as our inactivation results at 20 and 50 mg/L were very similar. The main hypothesis that explains this result is based on the direct oxidative effect of H_2O_2 and H_2O_2-derived ROS on internal organelles and the cell membrane, as well as the generation of hydroxyl radicals via internal Fenton reactions (Eqs. (1) and (2)) with intracellular free or loosely bound iron [28]. According to this hypothesis, the concentration of oxidative species and the frequency of oxidative attacks are responsible for bacterial destruction and inhibition, and these oxidative effects would be limited by the iron available inside the cells. Therefore, extra H_2O_2 will not necessarily produce better disinfection results. We observed this phenomenon in our results for H_2O_2/solar radiation treatment (Fig. 3); adding 50 mg/L of H_2O_2 did not improve the results compared to lower concentrations of H_2O_2. On the other hand, the addition of an appropriate concentration of hydrogen peroxide plays an important role in the inactivation when DOM is present in the water because the oxidation of DOM can compete with the inactivation of microorganisms [22].

All solar treatments that we tested for disinfection of RE gave very promising results (Fig. 8a and b). Furthermore, we found that Fe^{2+}/solar radiation treatment with 10 mg/L at pH 5 achieved levels below the DL in *E. coli* (5.44-log) and *E. faecalis* (5.26-log) after 4 h of treatment at 32.3 kJ/L. Different solar UV-A dosages accumulated in the sample (Q_{UV}) were needed to inactivate the different bacteria; *E. faecalis* required a higher Q_{UV} than *E. coli*. For both bacteria, the inactivation order was as follows: H_2O_2/Solar (50 mg/L) > photo-Fenton (10/50 mg/L of Fe^{2+}/H_2O_2) > H_2O_2/Solar (20 mg/L) > Photo-Fenton (10/20 mg/L of Fe^{2+}/H_2O_2) > Fe^{2+}/Solar (10 mg/L).

The best inactivation results for RE were obtained with 50 mg/L H_2O_2/solar treatment (Fig. 8). Photo-Fenton may have been worse than H_2O_2/solar treatment because the following factors were simultaneously in play: (i) The effect of precipitated iron at pH 5 (Table 3); the initially added iron quickly precipitated, so the concentration of dissolved iron was 0.3–0.2 mg/L at the end of the experiment. This produced loose iron and resulted in light screening by precipitated iron during the experiment. (ii) The competition of DOM and bacteria, as well as other microorganisms present in the RE, for the $OH^{\bullet}$ radicals generated during the photo-Fenton reaction. Despite these factors, when DOC reduction is considered, photo-Fenton treatment is much more effective than H_2O_2/solar treatment; we observed DOC reductions of 59.3% and 10.6% for the two treatments, respectively. SE contains simple organic matter, i.e., linear-chain organic compounds and aliphatic carboxylic acids (acetic, formic, propionic, pyruvate and maleic). These compounds are difficult to degrade by photo-Fenton processes. They are more difficult to mineralize than the organic matter present in RE, although the RE matrix has more ions and contains some suspended matter. This explains the better DOC degradation in RE compared to SE (Tables 2 and 3). Moreover, at near-neutral pH in RE, the presence of humic acids and other natural photosensitizers helps the iron to be active in the photo-Fenton reactions. This may not happen in an artificial water matrix that does not contain realistic types of organic matter [21].

In conclusion, very promising results were obtained by solar photo-Fenton treatment at pH 5 in RE samples. The complexity of applying these solar treatments to real effluents and wastewater lies in the chemical and microbiological compositions of the effluents. They contain a high organic and fecal load, and inorganic scavengers of hydroxyl radicals are present.

5. Conclusions

The main conclusions that can be drawn from this study are summarized below:

- Solar photo-Fenton treatment at pH 3 achieves complete inactivation of bacteria in SE with low dosages of solar UV energy. However, at pH 5, due to the precipitation of iron, the reaction rate decreases, and higher accumulated dosages of UV energy are needed to achieve good inactivation.
- Precipitated iron at pH 5 does not increase the generation of hydroxyl radicals via the Fenton reaction. The presence of precipitated iron gives an orange-brown shade to the water and slows the photo-Fenton treatment.
- The combination of hydrogen peroxide and solar irradiation provides an important synergistic effect for the inactivation of bacteria in SE and RE samples. The diffusion of hydrogen peroxide into cells causes the generation of hydroxyl radicals via Fenton reactions with intracellular iron. Proper hydrogen peroxide dosage provokes complete bacterial inactivation in water containing both organic matter and inorganic scavengers.
- *Escherichia coli* (Gram-negative) is more sensitive to the disinfection treatments than *Enterococcus faecalis* (Gram-positive). Therefore, the use of *Escherichia coli* as an indicator species for water disinfection studies should be reconsidered because efficient inactivation of *E. coli* by solar treatment does not necessarily imply the absence of other fecal bacteria.

- Solar disinfection treatments, such as solar photo-Fenton treatment and H_2O_2/solar treatment at pH 5, produce promising results for real wastewater effluent (RE). Complete bacterial (*E. coli* and *E. faecalis*) inactivation was achieved despite the complexity of the real wastewater matrix, which inherently has a variable chemical composition and contains large amounts of organic and inorganic matter.

Acknowledgements

The authors wish to thank the MICINN-FEDER for financing this research through the project "Regeneración de aguas depuradas mediante procesos de oxidación avanzada" (AQUASUN) (CTM2008-01876/TECNO). The authors also thank CAI-Programa Europa for a research grant and the Gobierno de Aragón for the PhD grant to Jorge Rodríguez-Chueca.

References

[1] M.A. Shannon, P.W. Bohn, M. Elimelech, J.G. Georgiadis, B.J. Mariñas, A.M. Mayes, Nature 452 (2008) 301–310.
[2] P. Dreschel, C.A. Scott, L. Raschid-Sally, M. Redwood, A. Bahri, Wastewater Irrigation and Health, Assessing and Mitigating Risk in Low-Income Countries, International Development Research Centre, Earthscan, London, 2010.
[3] USEPA, Guidelines for Water Reuse, U.S. Environmental Protection Agency, 2004.
[4] WHO, Guidelines for the Safe Use of Wastewater, Excreta and Greywater, Vol. 2: Wastewater Use in Agriculture, World Health Organization, Geneva, 2006.
[5] DM (185/2003) Regolamento recante norme tecniche per il riutilizzo delle acque reflue in attuazione dell'art. 26, c. 2, D. Lgs 11 maggio 1999, n. 152. Gazzetta Ufficiale.n. 169 del 23 luglio 2003.
[6] Queensland Water recycling Guidelines. Queensland Government, Enviromental Protection Agency, December 2005.
[7] Spanish Royal Decree 1620/2007 (BOE no 294, 8 December 2007). Concerns of the legal regime for the reuse of treated water.
[8] J.J. Gannon, M.K. Busse, Water Res. 23 (1989) 1167–1176.
[9] L. Moulin, F. Richard, S. Stefania, M. Goulet, S. Gosselin, A. Goncalves, V. Rocher, C. Paffoni, A. Dumètre, Water. Res. 44 (2010) 5222–5231.
[10] C. Levatensi, R. La Mantia, C. Masciopinto, U. Böckelmann, M. Ayuso-Gabella, M. Salgot, V. Tandoi, E. Van Houtte, T. Wintgens, E. Grohmann, Sci. Total. Environ. 408 (2010) 4923–4930.
[11] J. Rodríguez-Chueca, R. Mosteo, M.P. Ormad, M. Morales, J.L. Ovelleiro, Proceedings of 8th IWA International Conference on Water Reclamation & Reuse, Barcelona (Spain), 2011.
[12] J.W. Li, Z. Yu, X. Cai, M. Gao, F. Chao, Water Res. 30 (1996) 2371–2376.
[13] P.C. Singer, H.S. Weinberg, S. Krasner, H. Arora, I. Najm, American Water Works Association Research Foundation, Denver Co., 2002.
[14] G. Hua, D.A. Reckhow, Water Res. 41 (2007) 1667–1678.
[15] A. Dufour, M. Snozzi, W. Koster, J. Bartram, E. Ronchi, L. Fewtrell (Eds.), Assessing Microbial Safety of Drinking Water: Improving Approaches and Methods, WHO and IWA, London, UK, 2003.
[16] M. Lanao, M.P. Ormad, C. Ibarz, N. Miguel, J.L. Ovelleiro, Ozone Sci. Eng. 30 (2008) 431–438.
[17] M. Lanao, M.P. Ormad, P. Goñi, N. Miguel, R. Mosteo, J.L. Ovelleiro, Sol. Energy 84 (2010) 703–709.
[18] M. Lanao, M.P. Ormad, R. Mosteo, J.L. Ovelleiro, Sol. Energy 86 (2012) 619–625.
[19] C. Sichel, J. Blanco, S. Malato, P. Fernández-Ibáñez, J. Photochem. Photobiol. A Chem. 189 (2007) 239–246.
[20] M.I. Polo-López, P. Fernández-Ibáñez, E. Ubomba-Jaswa, C. Navntoft, I. García-Fernández, P.S.M. Dunlop, M. Schmid, J.A. Byrne, K.G. McGuigan, J. Hazard. Mater. 196 (2011) 16–21.
[21] D. Spuhler, J.A. Rengifo-Herrera, C. Pulgarín, Appl. Catal. B Environ. 96 (2010) 126–141.
[22] J. Rodríguez-Chueca, R. Mosteo, M.P. Ormad, J.L. Ovelleiro, Sol. Energy 86 (2012) 3260–3267.
[23] S. Malato, P. Fernández-Ibáñez, M.I. Maldonado, J. Blanco, W. Gernjak, Catal. Today 147 (2009) 1–59.
[24] M.I. Polo-López, I. García-Fernández, T. Velegraki, A. Katsoni, I. Oller, D. Mantzavinos, P. Fernández-Ibáñez, Appl. Catal. B Environ. 111–112 (2012) 545–554.
[25] J.J. Pignatello, E. Oliveros, A. MacKay, Crit. Rev. Environ. Sci. Technol. 36 (2006) 1–84.
[26] A. Moncayo-Lasso, J. Sanabria, C. Pulgarin, N. Benítez, Chemosphere 77 (2) (2009) 296–300.
[27] E. Ortega-Gómez, B. Esteban García, M.M. Ballesteros Martín, P. Fernández-Ibáñez, J.A. Sánchez Pérez, Catal. Today 209 (2013) 195–200.
[28] C. Sichel, P. Fernández-Ibáñez, M. de Cara, J. Tello, Water Res. 43 (2009) 1841–1850.
[29] F. Bichai, M.I. Polo-López, P. Fernández Ibáñez, Water Res. 46 (2012) 6040–6050.
[30] S. Goldstein, D. Aschengrau, Y. Diamant, J. Rabani, Environ. Sci. Technol. 41 (2007) 7486–7490.
[31] J.A. Imlay, Annu. Rev. Biochem. 77 (2008) 755–776.
[32] J. Marugán, R. Van Grieken, C. Pablos, C. Sordo, Water Res. 44 (2010) 789–796.
[33] M. Agulló-Barceló, M.I. Polo-López, F. Lucena, J. Jofre, P. Fernández-Ibáñez, Appl. Catal. B Environ. 136–137 (2013) 341–350.
[34] L.C. Navntoft, P. Fernández-Ibañez, F. Garreta, Sol. Energy 86 (2012) 307–318.
[35] P. Fernández, J. Blanco, C. Sichel, S. Malato, Catal. Today 101 (2005) 345–352.
[36] I. García-Fernández, M.I. Polo-López, I. Oller, P. Fernández-Ibáñez, Appl. Catal. B Environ. 121–122 (2012) 20–29.
[37] A.G. Rincón, C. Pulgarín, Appl. Catal. B Environ. 51 (2004) 283–302.
[38] P. Fernández-Ibáñez, C. Sichel, M.I. Polo-López, M. de Cara-García, J.C. Tello, Catal. Today 144 (2009) 62–68.
[39] C.A. Murray, S.A. Parsons, Chemosphere 54 (7) (2004) 1017–1023.
[40] A. Georgi, A. Schierz, U. Trommler, C. Horwitz, T. Collins, F.D. Kopinke, Appl. Catal. B Environ. 72 (1–2) (2007) 26–36.
[41] E. Lipczynska-Kochany, J. Kochany, Chemosphere 73 (5) (2008) 745–750.
[42] A.W. Vermilyea, B.M. Voelker, Environ. Sci. Technol. 43 (2009) 6927–6933.
[43] H. Xu, W.J. Cooper, J. Jung, W. Song, Water Res. 45 (2011) 632–638.
[44] Y. Chen, C. Hu, X. Hu, J. Qu, Environ. Sci. Technol. 43 (2009) 2760–2765.
[45] S. Canonica, U. Jans, K. Stemmler, J. Hoigné, Environ. Sci. Technol. 29 (1995) 1822–1831.
[46] C. Tixier, H.P. Singer, S. Canonica, S.R. Müller, Environ. Sci. Technol. 36 (2002) 3482–3489.
[47] S. Drakopoulou, S. Terzakis, M.S. Fountoulakis, D. Mantzavinos, T. Manios, Ultrason. Sonochem. 16 (2009) 629–634.
[48] C.J. Chung, H.I. Lin, C.M. Chou, P.Y. Hsieh, C.H. Hsiao, Z.Y. Shi, J.L. He, Surf. Coat. Technol. 203 (2009) 1081–1085.
[49] K.P. Kühn, I.F. Chaberny, K. Massholder, M. Stickler, V.W. Benz, H.G. Sonntag, L. Erdinger, Chemosphere 53 (2003) 71–77.
[50] A.I. Gomes, V.J.P. Vilar, R.A.R. Boaventura, Catal. Today 144 (2009) 55–61.
[51] L. Shaomin, G. Gaoli, X. Bihua, G. Wenqi, M. Guangjum, J. Wuhan, Univ. Technol. 24 (2009) 557–561.
[52] R. Van Grieken, J. Marugan, C. Pablos, L. Furones, A. López, Appl. Catal. B Environ. 100 (2010) 212–220.
[53] G. Fu, P.S. Vary, C.T. Lin, J. Phys. Chem. B 109 (2005) 8889–8898.
[54] K. Page, R.G. Palgrave, I.P. Parkin, M. Wilson, S.L.P. Savin, A.V. Chadwick, J. Mater. Chem. 17 (2007) 95–104.
[55] Y. Lan, C. Hu, X. Hu, J. Qu, Appl. Catal. B Environ. 73 (2007) 354–360.
[56] L. Villén, F. Manjón, D. García-Fresnadillo, G. Orellana, Appl. Catal. B Environ. 69 (2006) 1–9.
[57] T.N. Demidova, R. Hamblin, Antimicrob. Agents Chemother. 49 (2005) 2329–2335.
[58] B. Halliwell, J.M.C. Gutteridge, Biochem. J. 219 (1984) 1–14.
[59] M.I. Polo-López, I. Oller, P. Fernández-Ibáñez, Catal. Today 209 (2013) 181–187.
[60] D. Touati, M. Jacques, B. Tardat, L. Bouchard, S. Despied, J. Bacteriol. 177 (1995) 2305–2314.
[61] T. Nunoshiba, F. Obata, A.C. Boss, S. Oikawa, T. Mori, S. Kawanishi, K. Yamamoto, J. Biol. Chem. 274 (49) (1999) 34832–34837.
[62] G. López, M. Latorre, A. Reyes-Jara, V. Cambiazo, M. González, Biometals 25 (2012) 737–747.
[63] P.A. Bronstein, M.J. Filiatrault, C.R. Myers, M. Rutzke, D.J. Schneide, S.W. Cartinhour, BMC Microbiol. 8 (2008) 209.
[64] J. Ndounla, D. Spuhler, S. Kenfack, J. Wéthé, C. Pulgarín, Appl. Catal. B Environ. 129 (2013) 309–317.
[65] D.W.M. Gardner, G. Shama, J. Appl. Microbiol. 84 (1998) 633–641.
[66] M.I. Polo-López, I. García-Fernández, I. Oller, P. Fernández-Ibáñez, Photochem. Photobiol. Sci. 10 (2011) 381–388.